INLAND PENETRATION OF THE SEA BREEZE OVER THE SUBURBAN AREA OF TOKYO

HIROSHI YOSHIKADO and HIROAKI KONDO

National Research Institute for Pollution and Resources, 16-3 Onogawa, Tsukuba, Ibaraki 305 Japan

(Received in final form 19 April, 1989)

Abstract. Observational results of the structure of the sea breeze over the urban and suburban areas of Tokyo for four summer days are presented.

On two of these days, the inland penetration of the sea breeze front could be clearly traced. In one case, the sea breeze was first observed along the shores of Tokyo Bay around 0900 JST, and propagated in three hours through the Tokyo City area, the width of which is about 20 km. It then advanced inland at a rate of 16 km h^{-1}. Prior to the arrival of the sea breeze at the suburban site, the mixing height had remained at about 600 m for four hours. With the arrival of the sea breeze front, accompanied by an abrupt change in wind speed and direction, the mixing height increased sharply to 1700 m. It is suggested that this behavior and the structure of the front are intensified due to the urban effect, or the difference in the thermal characteristics between the urban and rural areas.

On the days without a sea breeze front, the land breeze system during the early morning was less intense, allowing the sea breeze to develop simultaneously with the inland valley wind and easily form a large-scale local wind system during the morning hours. In both cases, the vertical motion accompanying the local wind system works as a feedback mechanism to control the local winds by modifying the thermal and pressure fields.

1. Introduction

As for the vertical structure of the sea breeze, numerous observational data concerning the wind profile and its variation with time have been obtained from various areas of the world. However, the thermal structure of the sea breeze has not been documented so abundantly. As far as surface observations are concerned, it may be summarized that sea breezes transport cooler and moister air inland. An example in England presented by Simpson *et al.* (1977) showed a 1000 m mixed layer ahead of the sea breeze front and a stable moist layer with a thin superadiabatic surface layer behind it.

In this paper, some observational results of boundary-layer structure are given when the sea breeze advances inland from the shores of Tokyo Bay. The Kanto plain, which includes the Tokyo metropolitan area in the southern region, is the largest plain throughout Japan. The sea breezes that develop over the area have often been investigated with respect to the inland transport of atmospheric pollutants. Usually, several sea breeze systems interact with each other above the Kanto plain, and evolve in various patterns according to synoptic-scale meteorological conditions. Among them, one of the most important is the system that develops in Tokyo Bay and interacts with the valley wind systems in the mountainous western and northern regions, forming a large-scale local wind system in the late afternoon. This combined system transports air pollutants

Boundary-Layer Meteorology **48**: 389–407, 1989.

inland from the densely populated area around Tokyo Bay. Several observational and theoretical studies, e.g., Kurita and Ueda (1986) and Kimura (1985) have clearly described the process of the long-range transport of pollutants. Recent work by Ueda *et al.* (1988) attempted to explain the nighttime inland high concentrations of oxidants, with the sea breeze structure acting as a gravity current. Their study did not give sufficient data to show the characteristics of the gravity current but referred to the model by Simpson *et al.* (1977).

The sea breeze front observed in the present study showed a more notable structure than given by Simpson *et al.* (1977). That is, the sea breeze front was accompanied by a near neutral temperature profile that extended vertically much deeper than the inland mixed layer. The urban heat island effect is found to play a major role in forming the sea breeze structure with such a frontal configuration.

2. Data

Observations of the atmospheric structure up to 2000 m above the southern Kanto plain were carried out during the summer seasons of 1986 and 1987. The locations of the observation sites are shown in Figure 1. The terrain within the area covered by the observational network is very flat, and the farthest inland site Kumagaya (KUM) is about 30 m above sea level.

The urban area of Tokyo, where the ground surface is almost completely covered with man-made substances, extends roughly to the 10 km zone centered near the Kanda site (KAN). Outside of this, suburban residential areas change gradually to rural areas with distance, although even the rural areas are dotted with provincial cities. Urawa (URA) is a representative suburban site. KUM is also located in the suburban area of a moderate-size city, but the area surrounding the city consists of cultivated land. The distances from the shore of the bay to KAN, URA and KUM are 7, 30 and 68 km, respectively.

Data were obtained during three successive days each year. However, the first and second days of the 1987 period are excluded due to the local wind field being severely distorted by the passage of a synoptic-scale front. Therefore, the number of days analyzed in the present study is only four. Nevertheless, the data are considered to represent a typical developing process of the large-scale sea breeze system over the Kanto plain, since the synoptic pressure pattern was very typical for the summer season, with a large-scale sea breeze developing on each of the four days. An example of the synoptic pressure pattern is shown in Figure 2. As can be seen, a persistent high pressure system centered over the North Pacific extended over the Kanto district.

Radiosonde flights measuring dry- and wet-bulb temperatures were carried out five times (six times in some cases) a day during the period from 0600 to 1600 JST (Japan standard Time) at the sites KAN, URA and KUM. Tracking of pilot balloons (pibal) using the single theodolite method were carried out every hour, and at times every 30 min, during the same period of day as that of

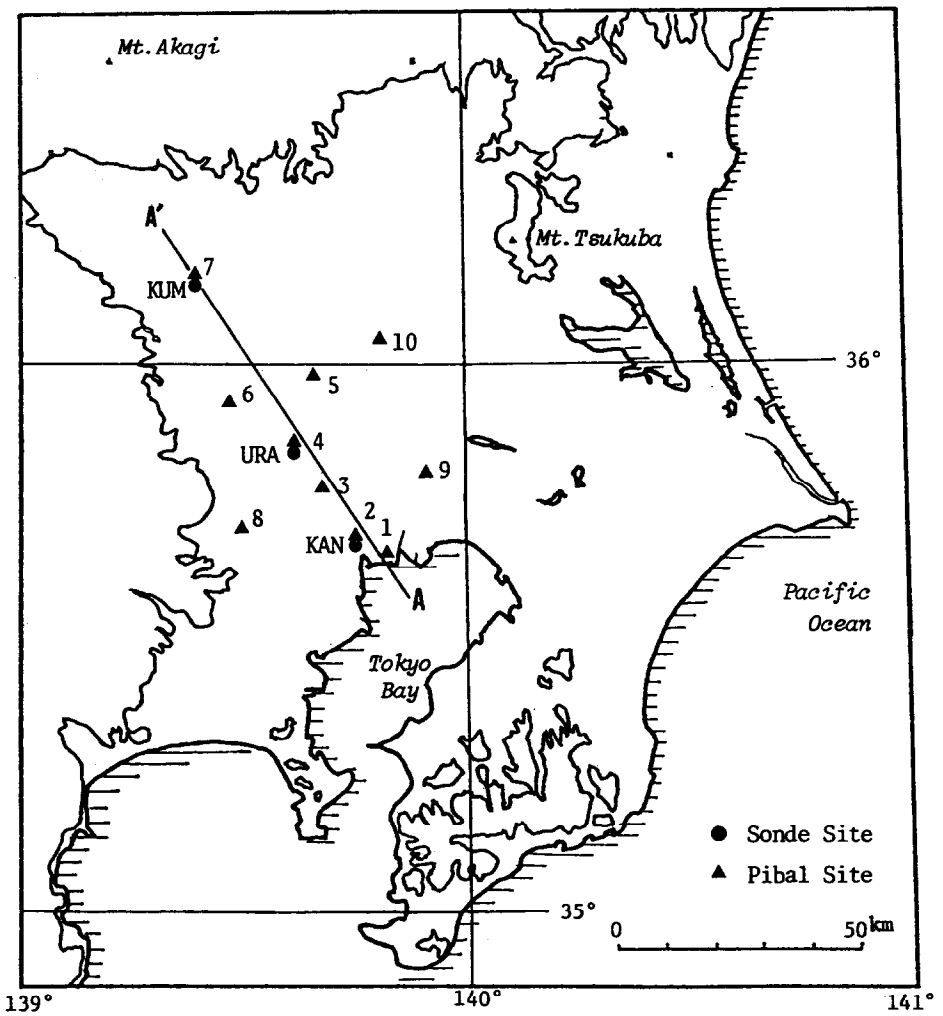

Fig. 1. Observational network. Site P1 is indicated by 1, P2 by 2, etc., and the contour represents 100 m above sea level.

radiosonde observations. The number of pibal sites was 10 during the 1986 observations indicated by P1–P10 in Figure 1, and 8 in 1987, excluding P8 and P10. The sites P2, P4 and P7 correspond to KAN, URA and KUM, respectively.

3. Results

3.1. Days with an apparent sea-breeze front

The observed sea breeze patterns can be divided into two groups, each containing two days. One is a 'frontal type' sea breeze, which is accompanied by

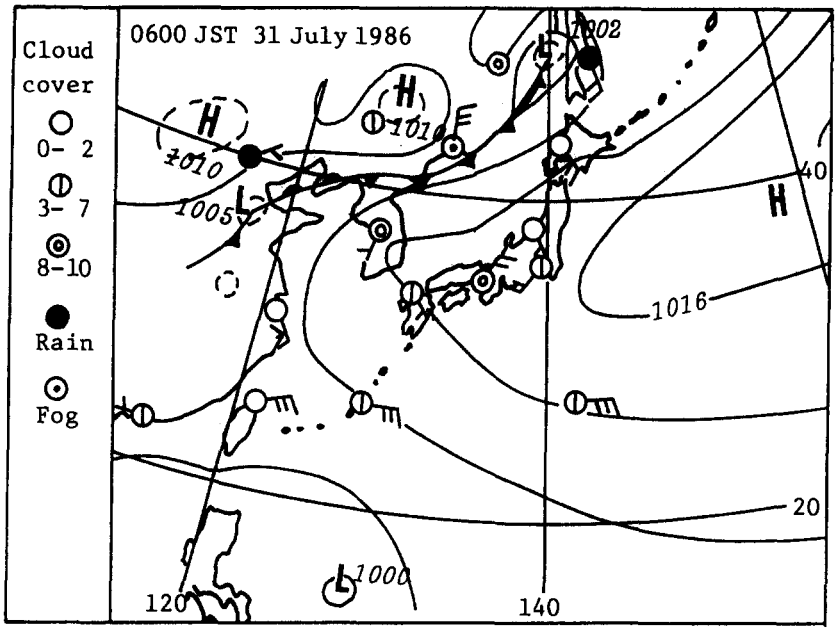

Fig. 2. An example of the synoptic pressure pattern for the day analyzed.

changes in the temperature profile, wind speed and direction when it reaches the inland sites. On 31 July 1986 and 20 August 1987, a sea breeze of this type was observed. The other is a 'non-frontal type', one in which these changes are not so apparent. On 29 and 30 July 1986, the latter was observed. For simplicity, hereafter, each day is identified by the number found in Table I.

In this section, the observational results of the frontal type sea breeze, mainly of Day 3, are presented.

(a) *Wind Field*

It can be seen in Figure 3 that a southwesterly wind indicated by G (hereafter, wind systems will be identified by symbols) was dominant over the coastal region

TABLE I

Numbering of the days examined

Number	Date	Sea breeze
Day 1	29 July 1986	non-frontal type
2	30 July 1986	
3	31 July 1986	frontal type
4	20 Aug. 1987	

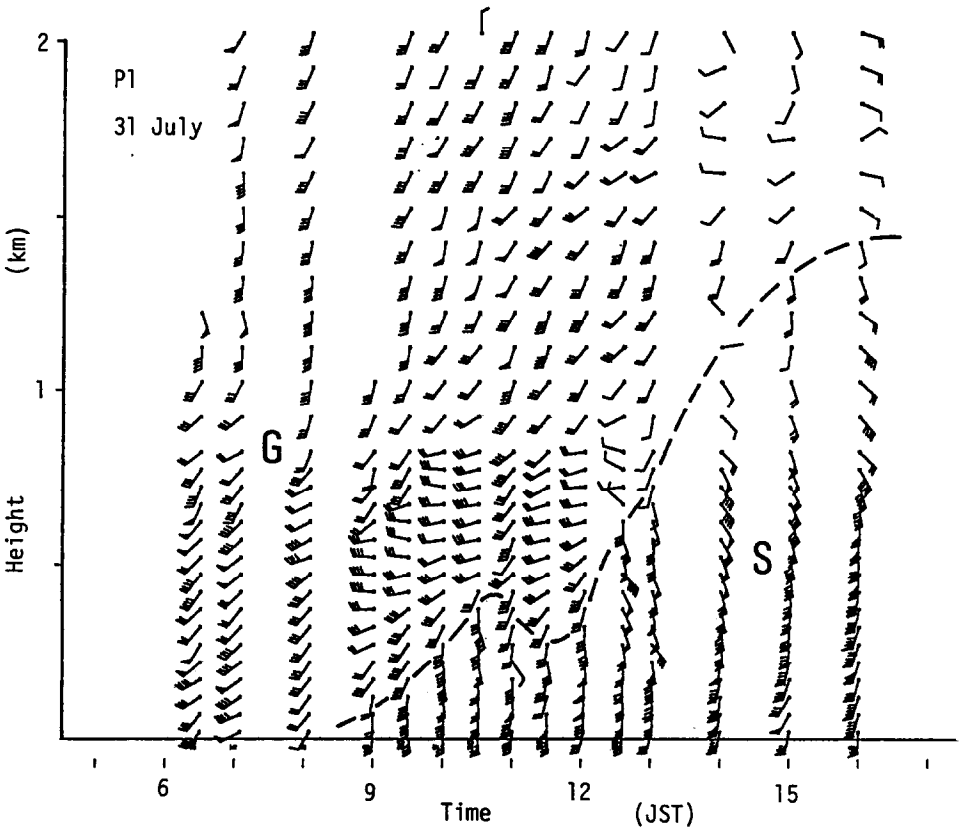

Fig. 3. Time-height cross-section of the wind above P1, 3 km north of the shore on Day 3. One wind barb indicates 1 m s^{-1}; one pennant 5 m s^{-1}.

in the morning. This wind system appeared every morning including the non-frontal days, and is consistent with the synoptic-scale pressure distribution (Figure 2). Although the equivalent geostrophic wind speed was about 8 m s^{-1} or less, G was so persistent that the land breeze that developed in the western and northern mountains could not penetrate to the coastal region. The onset of the sea breeze (S) at 0900JST is first recognized in the lowest layer as a slight shift in the wind direction. The depth of the sea breeze increased gradually up to about 1500 m in the mid-afternoon, though it was temporarily suppressed before noon by the wind system G being enhanced in the upper layer.

In contrast, the land breeze is distinctly recognized over the inland sites. One example is the wind direction changing from west to north with a depth of about 800 m found during the morning hours (L) in Figure 4. Similar winds were found in the data of the other three days. Around 1000 JST, a light wind period (T) with a somewhat variable wind direction began, and continued for about four hours. The sea breeze is detected as a strong southerly wind (S) at 1400JST. For

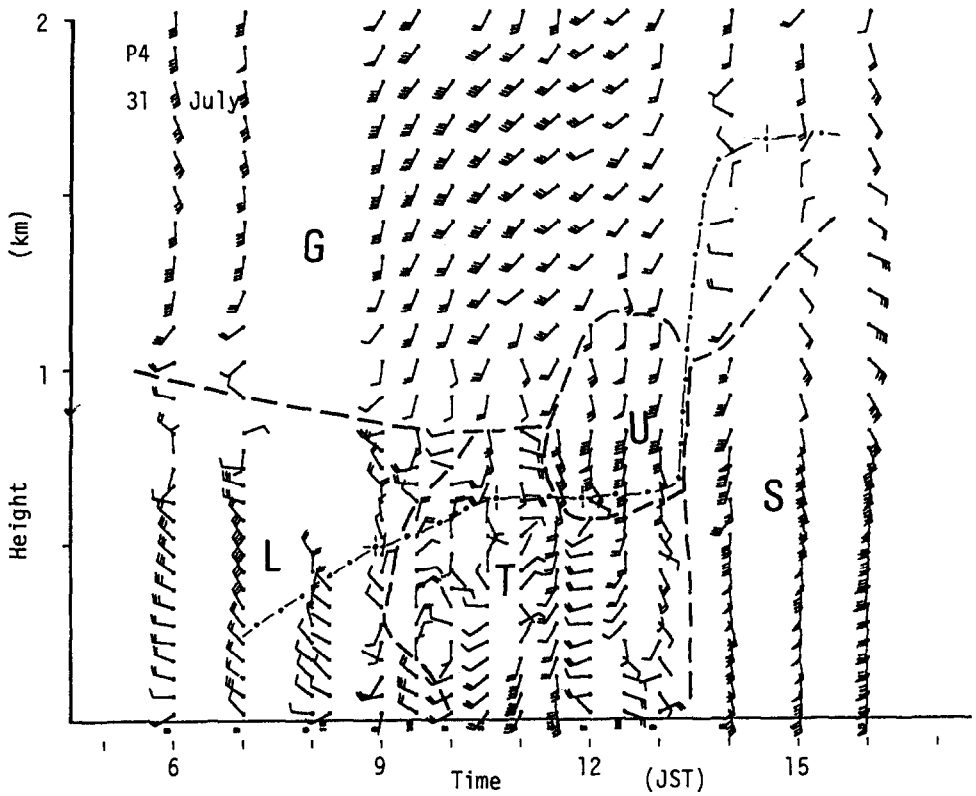

Fig. 4. Same as Figure 3 but for P4. The dash-dotted line indicates the height of the inversion base.

a few hours prior to that, however, a wind system (U) having the same wind direction as S is found above the T layer.

Figure 5 explains to some degree the character of U, although an exact evaluation is beyond the scope of the present study. A couple of closed circulations is found in the lower layer with an upward flow above Tokyo, and U is represented by the flow toward KUM at about 1 km above URA. Here, it is suggested that U may consist of three components: (1) the upper return flow of the urban heat-island circulation, (2) the leading edge of the sea breeze which slides over the suburban calm area, and (3) the lower portion of the synoptic-scale wind.

Figure 6 provides rough pictures of wind systems other than U in the horizontal direction. Here, the arrows are not very accurate in representing variations observed during the passage of a front since they are the result of interpolation with respect to time and space of the pibal data for a layer. One noticeable feature is that the wind direction in the T region became similar to that in the S region around 1200 JST. Its wind speed amounted to 8 m s^{-1} at P7 around 1400 JST. However, at the sites on the seaward side of P7, no corresponding high velocity wind was observed. This is described more clearly in

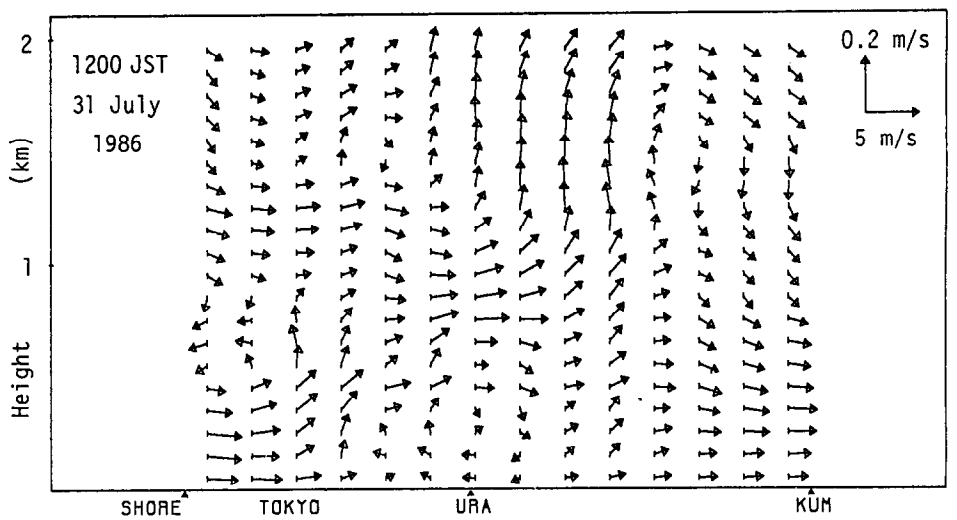

Fig. 5. Wind component in the vertical plane along A–A′ in Figure 1 at 1200 JST of Day 3. The wind on the grid was obtained from the pibal data through a simple interpolation procedure and a slight modification by means of the variational method (Sherman, 1978).

Figure 7. The sea breeze first appeared at the sites closest to the shore: P1 and P2 before noon. Next, it was found in the upper levels of the zone containing P3, P9 and P4. At the farthest inland sites, similarly, upper southerlies or easterlies were observed during the morning hours. These winds are not associated with the sea breeze by any means, but may be inland local systems induced by the topography. The extension of the sea breeze area can be traced by the subsequent sharp increases in wind velocity at the sites farther from the shore. The outline of the sea breeze area in Figure 6 is based on this analysis.

(b) *Thermal and Humidity Structure*

The potential temperature profile during the early morning shows a very stable stratification. The average gradient in the lowest 2000 m was roughly 0.01 Km^{-1}. This is associated with the fact that the predominant Pacific high covered the Kanto district (Figure 2), and is common in all the days examined.

After sunrise, a convective mixed layer grew at all radiosonde sites, but the process of the growth differs considerably. At KAN, a steady increase in mixing height continued (Figure 8) as long as wind system G flowed more or less parallel to the coastline; around 1030 JST, the sea breeze from Tokyo Bay arrived. As a result, the mixed layer was reduced and presumably changed into an internal boundary layer, the depth of which depends on the downwind distance from the shore. Actually, the depth and the potential temperature of the layer varied little after this time. Meanwhile, in the upper layer adjacent to the mixed layer, between heights of 600 and 1300 m, the potential temperature rose and the stable

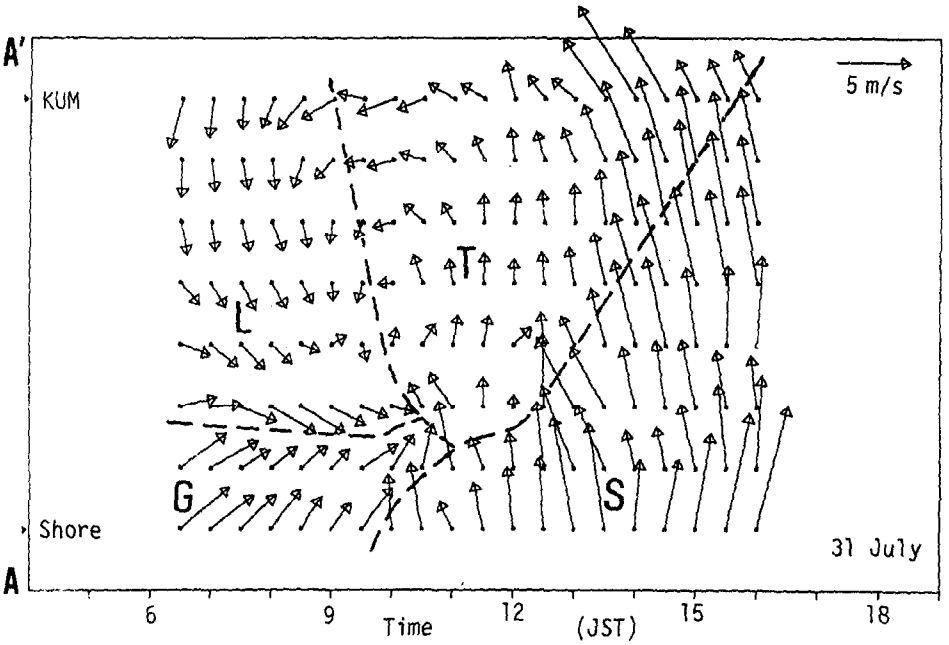

Fig. 6(a). Time variation of the wind in the layer 200–250 m above the surface interpolated to A–A' in Figure 1 for Day 3. An upward arrow indicates a southerly wind.

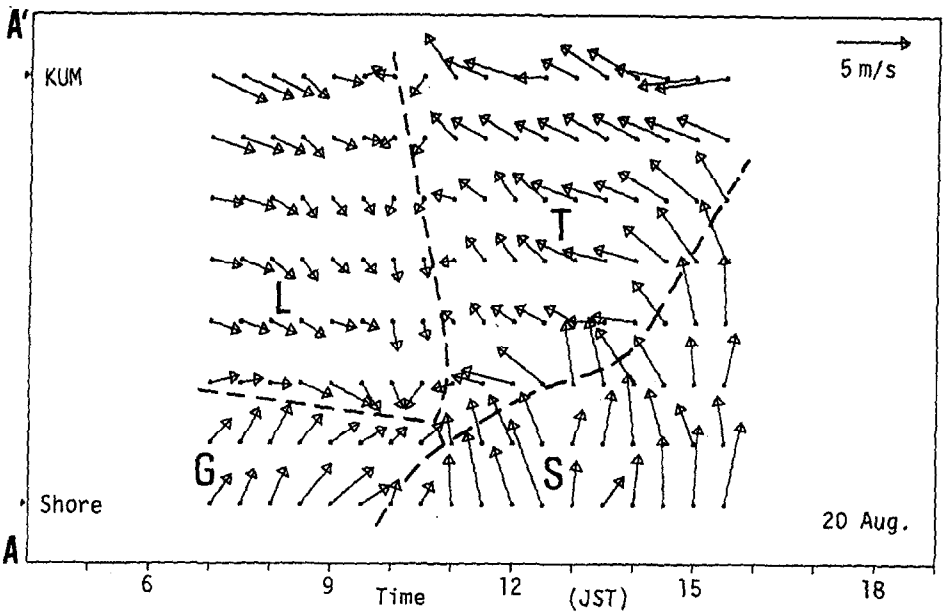

Fig. 6(b). Same as (a) but for Day 4 and in the 200–300 m layer.

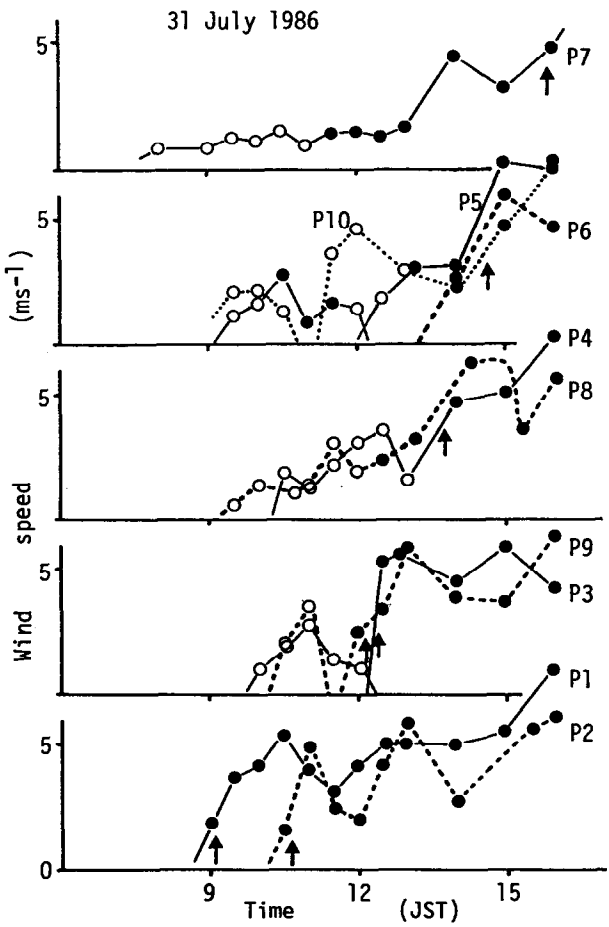

Fig. 7. Time variation of the average wind speed in a layer having a wind direction 80–190 deg from north but lower than 1050 m. Solid circles indicate wind systems close to the surface, and open circles upper ones. Upward directed arrows indicate inflow of the sea breeze.

stratification intensified, accompanied by a decrease in the specific humidity. These variations suggest that the sea breeze experienced downward motion in this zone. Furthermore, it is inferred that the sea breeze became rather dry by mixing with the upper dry air during its advance inland.

At URA, the rate of increase in the mixing height was very small between 0900 and 1200 JST. However, the sounding in the early afternoon shows that the mixing height has jumped to 1700 m (Figure 9), probably in acco · ' ınce with the invasion of wind system S (*cf.* Figure 4). Furthermore, anothe ıtral layer is found just above the inversion at the top of the mixed layer, before the arrival of S, which corresponds to the wind system U.

At KUM, the growth of the mixed layer was suppressed during the morning,

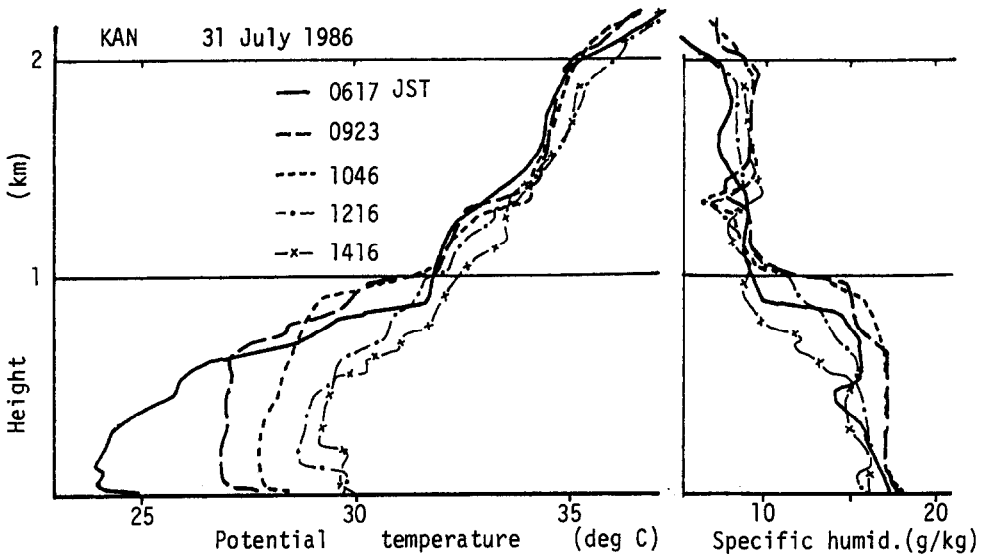

Fig. 8. Vertical profiles of potential temperature and specific humidity above KAN on Day 3. The times of the radiosonde release are indicated in the figure.

similar to that at URA. In the afternoon, the mixing height also increased, but the increase is not as remarkable. In addition, the sea breeze front had not reached KUM at the time of the latest sounding. Consequently, the rise in the potential temperature of the mixed layer was much higher than that at URA. At the same time, there was also heating in the upper layer. These variations suggest

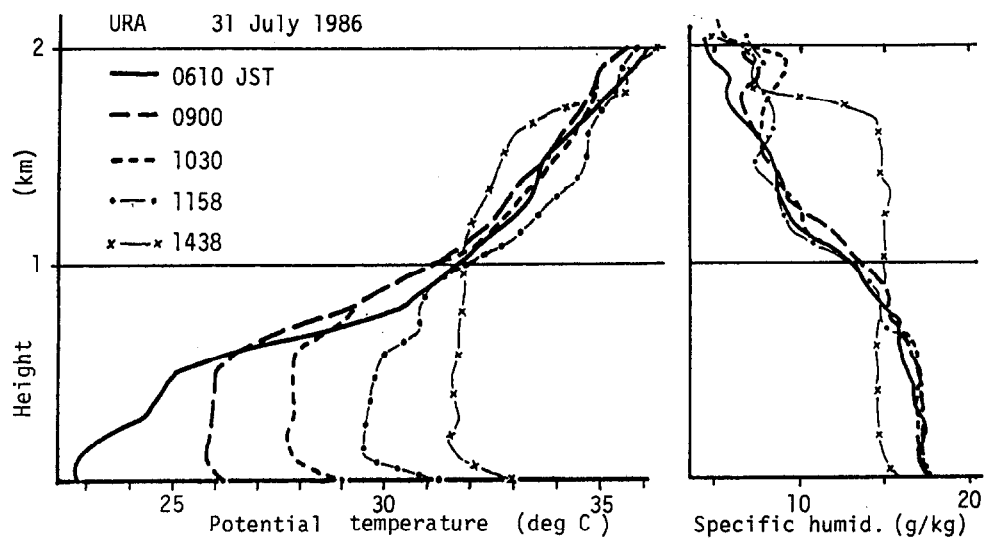

Fig. 9. Same as Figure 8 but for URA.

the existence of downward motion and entrainment of the warm upper air into the mixed layer. Calculations of divergence support this idea. Calculations from the upper winds at P4, P5 and P6, and also from P5, P6 and P7 reveal a distinct divergence on the order of $10^{-4}\,s^{-1}$, especially above the 800 m level over those inland areas after 1300 JST. The intensification of the inland wind system during the mid-afternoon at P7 mentioned in the previous section affects this result. The humidity profile also indicates that air has been supplied from the dry upper layers.

When the potential temperature profiles in Figures 8 to 10 are compared among the sites, the following relations are found. First, during the early morning around 0600 JST, the temperature of the surface layer was highest at KAN, probably due to the urban heat island effect. Above it, however, the temperature profiles were very similar up to 1000 m. In the layer between 1000 and 2000 m, temperatures became higher with distance from the shore. Second, the rise of temperature in the mixed layer during the morning was most notable at KAN, and was delayed inland. Third, the temperature at KAN stopped increasing due to the inflow of the sea breeze, and was overtaken by those at URA and KUM by noon. Fourth, around 1400 JST, warming of the mixed layer at URA stopped, or at least was slowed down by the passage of the sea breeze front, with strong cooling taking place in the upper layer, while heating continued at KUM, where the effect of subsidence added to the heating.

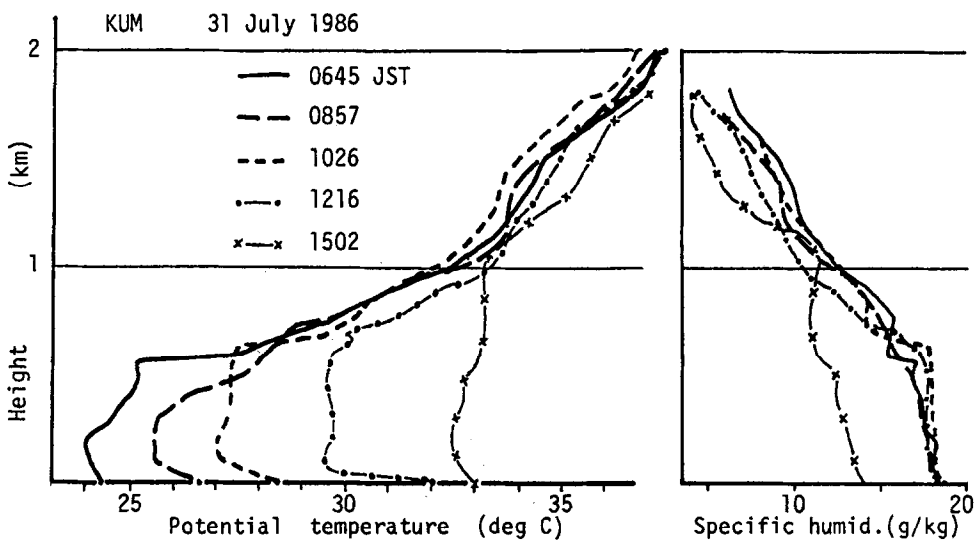

Fig. 10. Same as Figure 8 but for KUM.

(c) *Horizontal Pressure Gradient*

Variations in the pressure field correspond to variations in the thermal field mentioned above. The barometric records at the radiosonde sites cannot be used for the evaluation of horizontal pressure gradients because they were not sufficiently accurate and lacked the needed resolution. Instead, use is made of the pressure difference between the surface and 2000 m, denoted by ΔP, which was derived from the results of the radiosonde soundings through the pressure-height equation. Assuming that the pressure on the plane 2000 m above the surface is constant, the difference in ΔP will represent the difference in surface pressure. It can be seen from Figure 11 that ΔP differences among the sites were small during the early morning. As time passed, ΔP was reduced at KAN and KUM, and became relatively high at URA. This situation tended to prevent the advancement of the sea breeze from the shore to the northern suburbs of Tokyo, and to induce an inland southerly wind system. ΔP decreased at URA by noon and its difference from that at KAN vanished, allowing the sea breeze to extend into the suburban area. Furthermore, as ΔP at KUM was further reduced in the afternoon, the inland penetration of the sea breeze was enhanced.

When the temperature field mentioned in Section 3.1.(b) is taken into consideration, this case may be summarized as follows. The pressure gradient which caused the advance of the sea breeze front in the urban area near the shore is

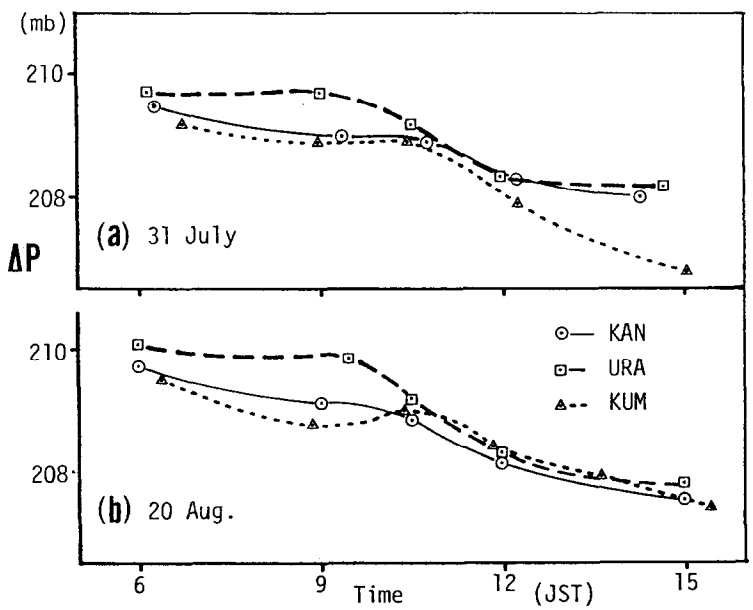

Fig. 11. (a) Variation with time of ΔP above KAN, URA and KUM on Day 3. (b) Same as (a) but for Day 4.

attributed not only to cooling by the sea breeze inflow itself, but also to the remarkable increase in the mixing height behind the sea breeze front. Here, the upper air was exchanged with cooler air causing a decrease in temperature. In contrast, in the inland area, the subsidence connected with the divergent wind field promoted a temperature rise. In addition to these observational results, the formation of a heat low centered in the mountainous region farther northwest of the present network area acted to enhance this pressure gradient (Kurita and Ueda, 1986).

To be more exact, the synoptic-scale pressure gradient must be taken into account. As a rough estimate, for example, from such weather charts as shown in Figure 2, the magnitude of the synoptic-scale pressure gradient was less than 10^{-2} mb km^{-1} and was directed from SSE to NNW. According to this condition, a slight pressure gradient from KAN to KUM should be superimposed on the pressure field represented by ΔP.

(d) *Another Example of the Sea Breeze Front*

In this section, the observational results of Day 4 are presented. The general structure of the wind systems is very similar to the foregoing case. For example, the sea breeze front remained for a few hours in the zone 10–20 km from the shore, and then advanced inland quickly (Figure 6(b)). These features are the same as in Figure 6(a) except that the processes were, on the whole, delayed by about one hour. The wind direction of the inland system within the T region was more from the east than from the south in the above case, but this difference is not essential for the present discussion.

The vertical profiles of potential temperature and specific humidity at URA, where the most remarkable variations were detected, are shown in Figure 12. The major characteristics are similar to those in Figure 9. A relatively high pressure zone formed over the suburban area in the morning (Figure 11(b)), as in the foregoing case. Heating presumably due to the subsidence associated with this high pressure system, occurred in the 1000–2000 m layer more distinctly than that for Day 3.

Concerning the data from KUM, one point should be mentioned. The phenomena observed in the former case such as the temporary intensification of the southerly wind around 1500 JST, the intense heating and the humidity decrease detected by the radiosonde released at 1502 JST were not detected at KUM on Day 4. On the contrary, the specific humidity in the upper layer increased in accordance with the rise in the mixing height. The less intense temperature rise may have coincided with the inflow of the above-mentioned easterlies, since easterlies were not clearly observed and the vigorous temperature rise lasted, as detected in the surface data, until 1600 JST at P6 which is adjacent to P7.

What has been stated regarding the pressure field for Day 3 shown in Figure 11(a) applies to Day 4 as well (Figure 11(b)). Differences in ΔP at the three sites

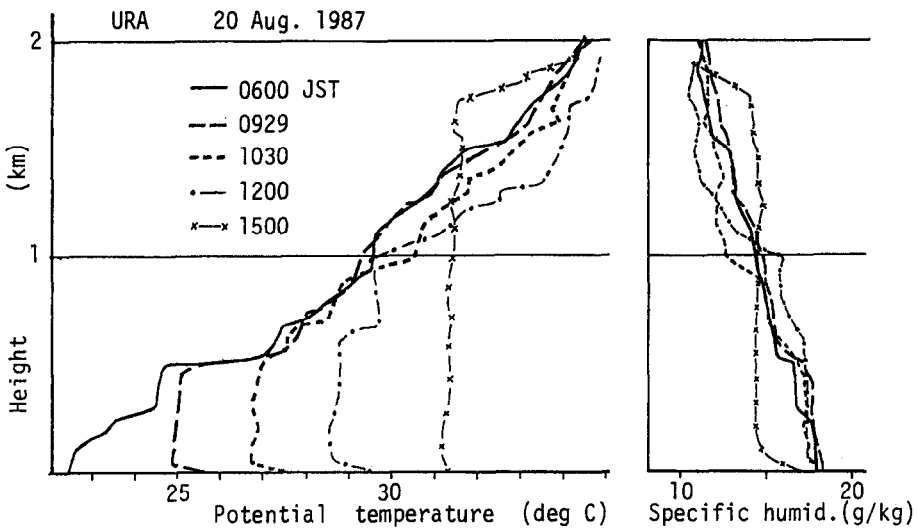

Fig. 12. Same as Figure 9 but for Day 4.

almost vanished in the afternoon, but the pressure decrease ahead of the sea breeze front, located near URA at 1500 JST, is believed to be larger for two reasons. First, the heating at KUM was not representative of this zone, the effective heating being more intense as mentioned of P6 above. Second, the synoptic-scale pressure gradient decreasing toward the northwest should be taken into consideration.

3.2. DAYS WITHOUT THE SEA BREEZE FRONT

(a) *Wind Field*

The wind variation above P1 is not very different from that in Figure 3. There, G changed to S around 0900 JST near the surface. At the suburban and inland sites, the difference from the frontal type days is conspicuous, an example of which is shown in Figure 13 in contrast to Figure 4. An inland wind system with wind direction from west to north occurred until 0900 JST or so in the layer 500–800 m above the surface at the western sites P3, P4, P6, P7 and P9. Surface winds at these sites were similar to those of the wind system G. A wind system similar to T appeared at some sites. However, it has the same wind direction as S, and the onset of S cannot be clearly determined. By early afternoon, S extended to P7.

(b) *Thermal Structure*

No essential differences are found in the characteristics of the vertical profiles of potential temperature and specific humidity above KAN from those of the frontal type days shown in Figure 8; however, the following two points are noteworthy.

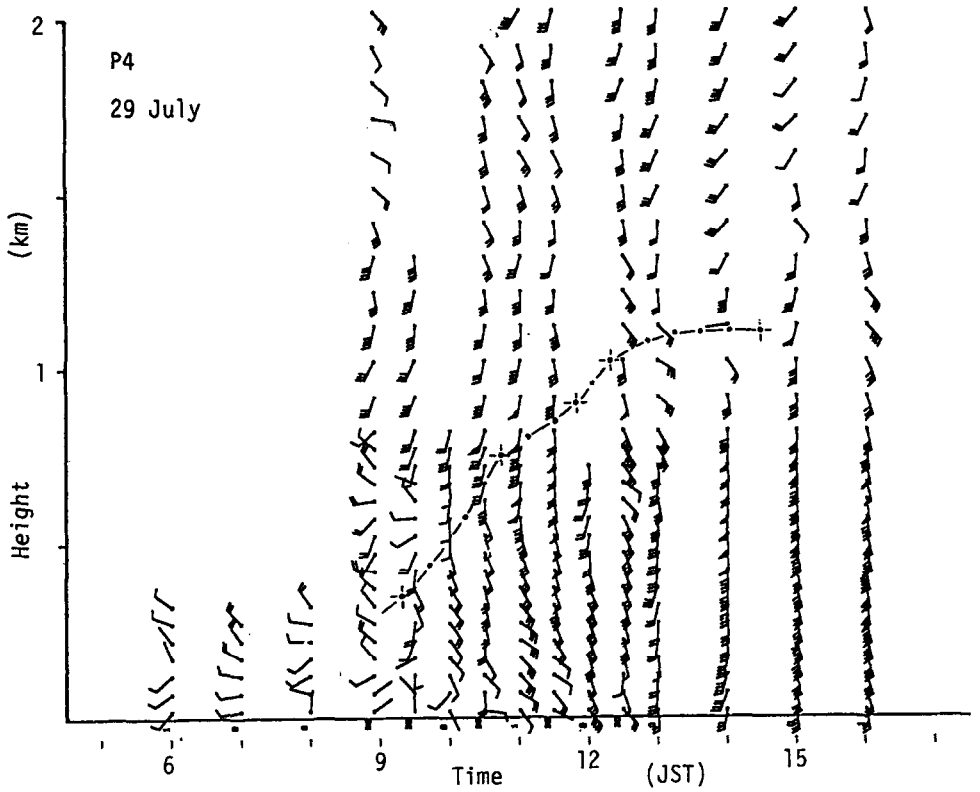

Fig. 13. Same as Figure 4 but for Day 1.

First, the mixed layer developed up to about 900 m around 1030 JST during frontal type days, while it had already begun to decay without reaching that level at that time for non-frontal days. This difference can be attributed to the fact that the onset of S at KAN occurred after 1000 JST in the frontal type days while it occurred before 1000 JST in the non-frontal case. Second, the temperature rise in the layer 1000–2000 m above the surface amounted to 0.5–1 K over approximately two hours after the 1200 JST sounding, a greater increase than in the former case. Upper level heating of a similar kind also occurred at URA. These were presumably caused by subsidence flow in the local wind system. The subsidence is not associated with the synoptic high because the temperature rise in the upper layer disappeared by the next morning. The upper level heating, relatively strong compared with the frontal type days implies the earlier establishment of a large-scale local circulation system.

The mixing height at URA exceeded 1000 m around 1200 JST in contrast with its restriction to lower levels until the sea breeze reached the site as in the former case. In the afternoon, however, the mixing height did not show signs of any increase although the potential temperature within the layer rose slightly.

At KUM, changes in the mixing height on Day 1 and Day 2 were not the same; its development was steady on Day 2 as in the case of URA, while it was retarded on Day 1 as was the case for frontal type days. However, this difference will not be further investigated in this paper.

(c) *Horizontal Temperature and Pressure Gradient*

Comparison of the potential temperature profiles at the three sites shows that conditions during the early morning were similar to that for the frontal type days. Namely, the nocturnal cooling in the lowest layer was small in the urban area, and that in the layer between 1000 and 2000 m was small in the inland area. This resulted in the largest ΔP at URA (Figure 14).

Around 0900 JST, the mixed-layer temperature at URA experienced a rapid increase and exceeded that at KUM, unlike the frontal type days. It even exceeded that at KAN by 1030 JST. As a result, the ΔP decreased at URA and became nearly equal everywhere. Due to this, it is likely that the synoptic-scale pressure field created a southerly wind over all the examined area. One reason why the mixed layer heating at URA was more rapid for this case is that clearer skies are considered to play an important role. The weaker land breeze system in the morning may have led to weaker vertical motion and less clouds.

During the afternoon, the rise in the mixed-layer temperature is most conspicuous at KUM. This, in addition to the stabilization of the upper-layer stratification, reduced ΔP to the lowest of the three sites. This condition is similar

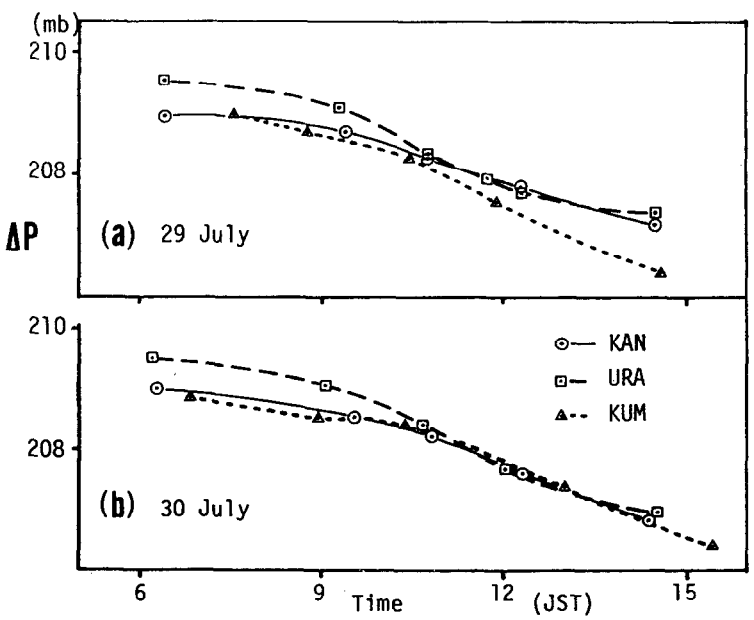

Fig. 14. Same as Figure 11 but for (a) Day 1 and (b) Day 2.

to the frontal type days. At KAN and URA, however, in contrast with the frontal type days, the reduction in ΔP during the afternoon was fairly large, especially on Day 2. For KAN, this was due to the greater heating in the upper stable layer as mentioned above. At URA, contrary to the upper cooling which occurred at the sharp increase in the mixing height for the case of the frontal type, heating similar to that at KAN contributed to the reduction in ΔP.

4. Summary

Observational results of the thermal structure of the sea breeze that arises from Tokyo Bay and penetrates inland through heavily urbanized areas have been presented. Although the number of cases examined is small, the synoptic weather conditions under which they occurred are very typical for summer in this region.

The onset of the sea breeze at the shore occurred around 0900–1000 JST. Simultaneously, the inland wind began to shift from northwest to southeast. This implies a decay in the land breeze regime and the formation of the valley wind system. Both systems are related to the inland terrain. In fact, even the land breeze, in spite of the impression that it is related to a land-sea contrast, has its origins in the mountainous areas and often proceeds eastward or southward over the Kanto plain with a frontal-like structure (Fujibe, 1985).

Although the wind direction of the sea breeze is not very different from that of the inland valley wind, the inland penetration of the sea breeze area can be traced during the frontal type days. The advent of the front is clearly detected by the sharp increase of mixing height and the change in the wind direction deep in the boundary layer as well as the sudden change in the wind velocity.

The fact that the advance of the sea breeze front was much slower over the heavily urbanized area than over the surburban and rural areas is mainly related to the urban heat island. That is, in the urban area the nocturnal cooling was less, the temperature rise and the mixed-layer growth during the morning hours were greater, and therefore, the pressure in the lowest layer became lower by about 0.7 mb than in the suburban area. Roughness, which has larger values in the urban areas, may also be an important factor that retarded the sea breeze advance. Taking these factors into account, it is considered that vertical motions induced by the change in the wind in the lowest layer, through the modification of the temperature and pressure fields, controlled the sea breeze.

While the sea breeze front was over Tokyo, the mixing height in the suburban and rural areas remained at 600–700 m and the wind within this layer was not steady. Above the mixed layer, a southerly wind region with a nearly constant potential temperature appeared. This can be traced back to the region of high temperature above Tokyo.

When the sea breeze front advanced to the suburban area, the mixing height experienced a sharp increase to about 1700 m. This abrupt change was not caused by an intensification in the heating and mixing, but by the upheaval of sea

air. As a result, the potential temperature in the upper portion of the deepened mixed layer decreased, and resulted in a temporary rise of surface pressure, or at least prevented the surface pressure from decreasing further. In other words, if the sea air is not accumulated to a sufficient height, it cannot break through the suburban high pressure zone formed during the morning hours.

Since the sharp increase of the mixing height was not a result of a normal developing process of the mixed layer but was an exchange of air masses, the arrival of the front corresponded to an increase in the concentration of pollutants in the upper layer between 700 and 1700 m without a decrease in the lower layer (Yoshikado and Yamamoto, 1988). However, detailed analysis of pollutants has been excluded from the present study. The specific humidity also displayed a sudden increase in the upper layer at the passage of the front, while it rather decreased in the lower layer. This implies that the sea air was drier than the inland mixed-layer air due to the entrainment of dry upper air over the shore area.

In the mid-afternoon when the sea breeze front passed through the suburban and inland areas, the heat supply from the underlying surface began to decay, so that the deepened mixed layer behind the front could not maintain itself very long, and was easily modified by advection. The potential temperature profile for 1430 JST on Day 3 above URA appeared to show such a situation, as the frontal passage occurred at this location about 30 min earlier.

Takano (1977) studied the influence of anthropogenic heating and the surface properties over the Tokyo metropolitan area on the sea breeze using a 3-dimensional numerical model. General features analyzed in the present study coincide well with model-calculated results. For example, the interruption of the inland penetration of the sea breeze by the urban heat island and the downward motion over the inland area correspond rather well. Also, the mixing height over the urban area of ~1500 m and that over the inland area of ~800 m agreed, although the vertical gradient of potential temperature was 0.005 Km^{-1} in the model, smaller than the observed results. Furthermore, the model calculation neglected the terrain for the mountainous areas far inland and did not sufficiently describe the process of the inland penetration of the sea breeze. Advanced numerical models (Kimura, 1985 and Kondo, 1989) have been applied to the sea breeze over the Kanto plain, but did not focus on the urban heat island effect influencing the sea breeze structure.

For the days with the non-frontal type sea breeze, the land breeze in the early morning was relatively weak and the synoptic-scale southerly flow appeared to dominate from the early morning hours. This does not mean that a predominant synoptic-scale southerly flow is a necessary condition for the non-frontal type sea breeze. In order to investigate the criteria for frontal type and non-frontal type sea breezes, a statistical analysis consisting of many more sample days is required. Then, in addition to the intensity and direction of the synoptic-scale wind, the heat island effect of Tokyo may also be found to be an important modifying

factor. In the examined case, the wind shift from the synoptic-scale southerly flow to the sea breeze was small, and almost simultaneously the inland valley wind system occurred. The appearance of a distinct boundary such as a front cannot be found between them. In the suburban area, the mixing height increased steadily up to 1000 m during the morning hours, while it showed no further development in the afternoon. This variation is in remarkable contrast with that of the frontal type days.

In all cases, the vertical motion played an important role in the local wind mechanism. Judging from the rate of mixed-layer growth and the temperature variation in the upper layer, the upward flow was concentrated in the frontal zone and presumably over the inland mountainous area, and descending flows prevailed above the other areas during the afternoon. These vertical motions affected the mixing height, the temperature profile and the pressure distribution, and controlled the local winds as a feedback mechanism. Quantitative evaluation of these processes is to be investigated in a subsequent study.

Acknowledgements

The authors wish to express their thanks to Dr. O. Yokoyama and Dr. K. Kitabayashi of the National Research Institute for Pollution and Resources for their coordination of the observation program.

References

Fujibe, F.: 1985, 'Air Pollution in the Surface Layer Accompanying a Local Front at the Onset of the Land Breeze', *J. Meteorol. Soc. Japan* **63**, 226–237.

Kimura, F.: 1985, 'A Numerical Simulation of Local Winds and Photochemical Air Pollution (II): Application to the Kanto Plain', *J. Meteorol. Soc. Japan* **63**, 923–936.

Kondo, H.: 1989, 'Description of NRIPR Mesoscale Model', *Report Nat. Research Inst. Pollution and Resources*, No. 44.

Kurita, H. and Ueda, H.: 1986, 'Meterological Conditions for Long-Range Transport under Light Gradient Winds', *Atmos. Environ.* **20**, 687–694.

Sherman, C. A.: 1978, 'A Mass-consistent Model for Wind Fields over Complex Terrain', *J. Applied Meteorol.* **17**, 312–319.

Simpson, J. E., Mansfield, D. A., and Milford, J. R.: 1977, 'Inland Penetration of Sea-Breeze Fronts', *Quart. J. Roy. Meteorol. Soc.* **103**, 47–76.

Takano, K.: 1977, 'Three Dimensional Numerical Modelling of the Land and Sea Breezes and the Urban Heat Island in the Kanto Plain', Dr.Sci. Thesis, Tokyo University.

Ueda, H., Mitsumoto, S., and Kurita, H.: 1988, 'Flow Mechanism for the Long-Range Transport of Air Pollutants by the Sea Breeze Causing Inland Nighttime High Oxidants', *J. Applied Meteorol.* **27**, 182–187.

Yoshikado, H. and Yamamoto, S.: 1988, 'Inland Transport of the Atmospheric Pollutants over Tokyo by the Sea Breeze', *Preprints of 14th Conference on Industrial Pollution*, Agency of Industrial Science and Technology, Japan, 122–123 (in Japanese).